

# STOCHASTIC SIMULATIONS WITH APPLICATIONS IN MATERIAL SCIENCES

Deák Robert  
Theses of the Ph.D. Dissertation

Joint Ph.D. supervision between:



Department of Physics  
Babeş–Bolyai University, Cluj-Napoca, Romania  
Scientific advisor: Dr. Néda Zoltán, D.Sc., professor, external member of HAS

and



Department of Materials Physics  
Eötvös Loránd University, Budapest, Hungary  
Scientific advisor: Dr. Groma István, D.Sc., professor

Graduate School of Physics  
Doctoral Program for Material Science and Solid State Physics  
Head of School: Dr. Palla László, D.Sc., professor  
Head of Program: Dr. Lendvai János, D.Sc., professor

Cluj–Napoca, Romania

2013

# Introduction

Nowadays, several deposition technics are used for the production of thin films and coatings, like the Physical Vapor Deposition (PVD) [5], the Chemical Vapor Deposition (CVD) [5], the Molecular Beam Epitaxy (MBE) [6, 7], and the hybrid methods that are combinations of the different technics [5]. The variety of vapor deposition technics also show the multiplicity of applications of thin films. They are used in the industry of integrated circuits, displays, hard disk drives, magnetic memories, large area detectors; in reducing the friction coefficient of surfaces; to improve wear resistance of gas turbine engines; to grow nanoscale particles with practical interest, and many other applications (for reviews see [5, 8]).

Because of the increasing interest in thin films, this area of Material Science is widely studied. In the last two decades several experimental and theoretical studies were carried out in order to understand the various surface phenomena like surface diffusion of atoms and atomic clusters, island nucleation and growth, island coalescence and Ostwald ripening, simultaneous deposition of different types of atoms, morphology of two-dimensional islands formed by the deposited atoms, etc.

The process where crystals are grown on crystalline surfaces by the deposition of atoms in vacuum is called epitaxial growth. Typically, the deposition rate is small and the crystal is grown, loosely speaking, one layer at a time. In the specific case of deposition from vapor it is well-known that individual atomic events can strongly influence and even dominate the final micro or nanostructure of epitaxial thin films. Over the years, experimental technics like Scanning Tunneling Microscopy (STM), in-situ Transmission Electron Microscopy (TEM), Field Ion Microscopy (FIM), and Reflection High-Energy Electron Diffraction (RHEED) have mostly been carried out on clean, low-index metal surfaces at low temperatures, to study the individual atomic events of surface phenomena. In spite of modern visualization tools in the experiments, the researchers are still not able to identify the atomic processes responsible for surface diffusion. Because of the very fast nature of atomic diffusion it is hard to explain and give a detailed picture of the observed and studied processes. To overcome the experimental difficulties, several theoretical and computational technics were developed, like

Molecular Dynamics (MD), first-principle (or ab-initio) calculations, Monte Carlo (MC) methods, static calculations, effective medium theory calculations, and many hybrid methods, combining the different technics. As the different vapor deposition technics have their own strengths for creating thin films with specific properties, also the theoretical and computational technics have their own strengths and weaknesses in calculating or simulating specific properties or phenomena with different accuracy or speed. For example, it is known that MC methods are much weaker approximations to reality than the nowadays fashionable ab-initio MD simulations, but on the other hand, with MC methods we are able to simulate much larger systems for much longer dynamical time, as long as with ab-initio MD the simulated time and system size is much more reduced.

Using these theoretical and computational methods one could better understand the atomic processes and also shade light on the effects of the experimentally controllable parameters, and therefore one can engineer structures with the desired practical properties.

The aims of our work were to study thin film growth related questions and problems by using two original kinetic Monte Carlo methods developed by us (kMC method A and kMC method B).

The first chapter of the dissertation reviews the main three categories of computational technics: the deterministic models, the stochastic models and the hybrid models. The second chapter is devoted to present the developed original kinetic Monte Carlo (kMC) methods and their motivating studies. The third chapter discusses the applicability of the developed methods presenting and discussing the obtained results. After the final conclusions, a comprehensive bibliography for this subject is given.

# Methods

During our work I used both analytical methods and computer simulations to calculate qualitative and quantitative properties of thin film growth related phenomena.

We have developed two original kinetic Monte Carlo (kMC) methods.

The **kMC method A** improves the classical kMC method by using a new hopping barrier formula and incorporating more degrees of freedom for the diffusion of particles. The latter is achieved by considering a triangular lattice topology and taking into account both the Face Centered Cubic (FCC) and the Hexagonal Close Packed (HCP) sub-lattice sites. A Lennard-Jones type pair-potential was used for handling the interactions between the particles. With this kMC method the two-component co-deposition process was successfully modeled, using a reduced number of parameters. Impurity decorated islands were formed without using a predefined rate for direct exchange of the neighboring particles. Also, for the homo-epitaxy problem the island growth, the coalescence, the appearance of stacking-faults related phase-boundaries and their motions were all successfully reproduced. This method is computationally fast and systems with tens of thousands of atoms can be simulated in reasonable computational time on PC type computers [1, 2].

The **kMC methodB** is an improvement of the first method and performs a more accurate calculation of hopping barriers by using the Nudged Elastic Band method (NEB) [9, 10]. The interaction of the particles are calculated with the generalized Embedded Atom Method (gEAM) [11]. By using gEAM it is possible to study material-related problems and quantitatively compare the results with those from experiments and from ab-initio calculations. Using this method I studied the statistics of the diffusion of Pt atom clusters on a Pt(111) surface [3].

Also, using the kMC method B, I have analyzed the formation and stability of the oriented triangular Pt islands on Pt(111) surfaces [4].

# New scientific results

Thesis 1: *The hopping barrier for the atomic diffusion process in many thin film related studies - using the classical kMC method - is either a phenomenological energy barrier or simply the binding energy of the particle at the starting position of the jump. For the sake of simplicity and faster calculations, usually a square lattice is used. In order to improve the classical kMC method, we developed the kMC method A. This method uses the triangular lattice, leaving the particle to occupy both the FCC and HCP sub-lattice sites, and calculates the diffusion hopping barrier by taking into account the binding energies in the initial and also in the final states. Using the simple and fast kMC method A, I have studied the time-evolution of island growth. The results are in qualitative agreement with experimental data. I also reproduced for island coalescence the realistic formation of necks and fast rounding of the resulted islands. Also, for homoepitaxial deposition I have successfully studied the formation and realistic dynamics of stacking-faults related phase boundaries. We found that the phase boundaries swings, trying to keep their length as short as possible and ultimately disappear with the disappearing HCP islands.*

As a first study, using the fast kMC method A, we investigated the time-evolution of homo-epitaxial island nucleation and growth phenomena and qualitatively compared the simulation results with the experimental results.

Using the kMC method A, the only phenomenologic energetic parameter is  $E_{AA} = 0.15eV$ , the interaction energy at equilibrium distance ( 1 lattice constant) between the same type of atoms (type A). The fixed parameters for the simulations were the temperature,  $T = 550K$ , the deposition rate,  $F = 10ML/s$  and the attempt rate  $f_0 = 10^{12}Hz$ , which is roughly the vibration frequency of atoms in a crystal. Systems with  $512 \times 512$  size were considered and the time-evolution of the average island sizes was qualitatively compared with the results of an in-situ transmission electron microscopy experiment for Indium deposition on amorphous Carbon membrane, obtained in the MFA- KFKI (Budapest, Hungary) laboratories [12]. Eperiments are for three-dimensional islands while simulations are for simple monolayers. In spite of differences a qualitative agreement is observable in

the trends (Figure 1). The shape of the curves are quite similar.

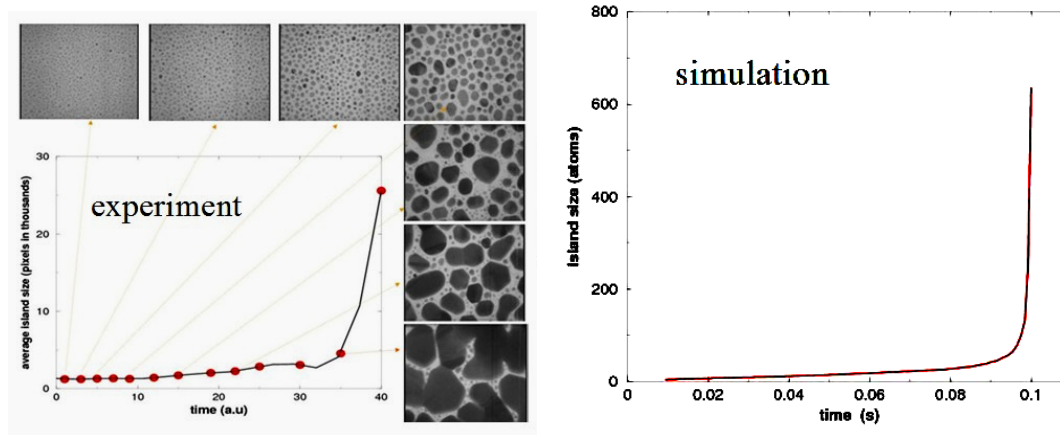


**Figure 1:** *Experimental and simulated trend of the average island size as a function of time during the formation of a continuous covering layer. Simulations are for  $T = 550K$  and  $F = 10ML/s$  deposition rate.*

Considering the case when atoms are deposited with a fixed deposition rate ( $F = 10ML/s$ ) on a planar FCC (111) surface formed by the same type of atoms, similar to the previously discussed case, monolayer domains of the two equivalent orientations but with different, FCC and HCP sequences can nucleate and grow.

Using the kMC method A, the formation, motion, and annihilation of stacking-faults related phase-boundaries can be followed in time (Fig. 2). Although the FCC and HCP sites are geometrically equivalent, using this method the binding energy is slightly different. Because the FCC sites are energetically lower, as the time evolves, the HCP islands slowly disappears resulting in FCC type islands as one can conclude from Figure 2.

Coalescence is by definition the process in which islands merge together. The scenario for islands coalescence obtained by simulations using the kMC method A is in qualitative agreement with the one observed in experiments. From simulations it is observable the realistic formation of necks and the fast rounding of the resulting islands. A simulation sequence in this sense is illustrated in Fig. 3. Movies made from simulation results are available on the home-page dedicated to this study [13].

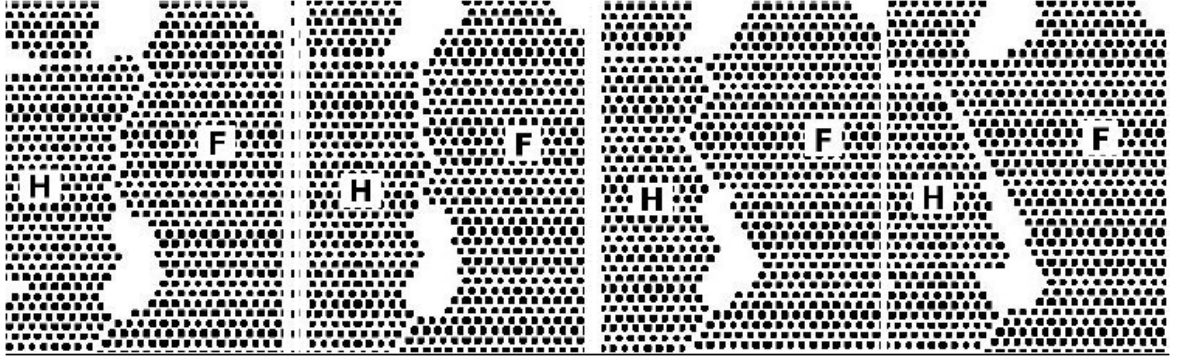


**Figure 2:** Characteristic time evolution and annihilation of stacking-faults related phase-boundaries for the case of homoepitaxial deposition. The pictures from left to right represent steps in the time-evolution. The *F* and *H* islands corresponds to FCC and HCP stackings, respectively. Simulation parameters are:  $E_{AA} = 0.15\text{eV}$ ,  $T = 650\text{K}$ ,  $F = 10\text{ML/s}$  and  $f_0 = 10^{12}\text{Hz}$ .

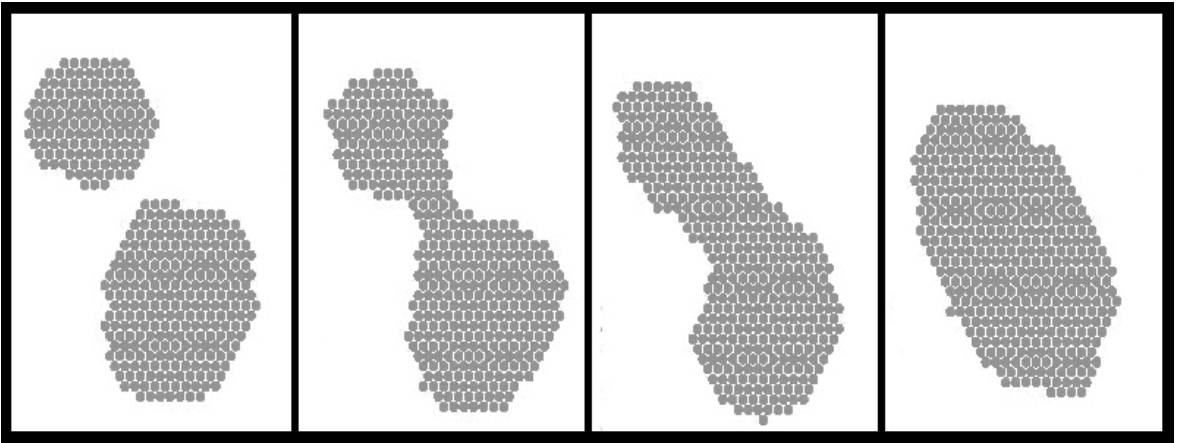


**Figure 3:** Snapshots from simulated island coalescence. Simulation parameters are:  $T = 450\text{K}$  and  $F = 0.1\text{ML/s}$ .

Thesis 2: Using the classical kMC method for two component co-deposition, previous studies proved that an energetic bias favoring segregation is not sufficient to obtain impurity decorated islands. To achieve this segregation, a thermally activated exchange mechanism has to be introduced between the different type nearest neighboring atoms, by postulating a phenomenological direct exchange barrier. We showed that using the kMC method A without considering a phenomenologically predefined direct exchange rate it is possible to reproduce the segregation process in which impurities are decorating the growing islands.

The two component co-deposition process was also successfully modeled using the kMC method A. The exchange mechanism between atoms of different types being on neighboring lattice sites appears directly from diffusion without considering an artificially predefined rate

for such a process. This non-realistic ingredient was necessary in previous studies in order to obtain impurity decorated islands. By using kMC method A, it is possible to simulate with a reduced number of parameters the special segregation process in which impurities are decorating the growing islands. In this case the only phenomenologic energetic parameters are  $E_{AA}$ ,  $E_{BB}$  and  $E_{AB}$ , which are the interaction energy at equilibrium distance ( 1 lattice constant) between the same and different types of atoms.

For the fixed parameters  $f_0 = 10^{12}Hz$ ,  $E_{AA} = 0.15eV$ ,  $E_{BB} = 0.0001eV$  and as a function of the  $E_{AB}$  parameter (varied in the  $0.02 - 0.12eV$  interval) two main types of structures were observed: (i) island containing intermixed type  $A$  and  $B$  atoms, and (ii) islands decorated by  $B$  impurities. As expected, for low  $E_{AB} < 0.08eV$  values the impurity decorated islands are stable, while for higher  $E_{AB} > 0.08eV$  values the islands containing intermixed type  $A$  and  $B$  atoms are observable. This is illustrated in Figure 4.

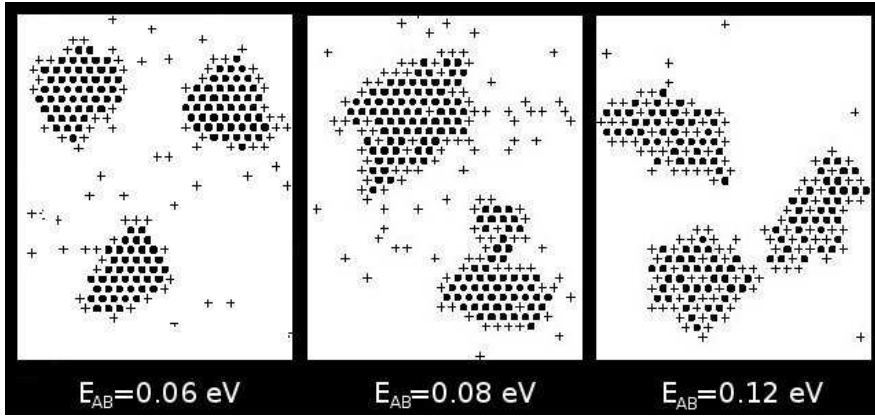


**Figure 4:** Island structures obtained as a function of the  $E_{AB}$  parameter. Simulations done for  $E_{AA} = 0.15eV$ ,  $E_{BB} = 0.0001eV$ ,  $T = 650K$ ,  $F_A = F_B = 10ML/s$  and  $f_0 = 10^{12}Hz$ . The structures from left to right are obtained for  $t = 1.25 \times 10^{-2}s$  (60000 MC steps),  $t = 2.73 \times 10^{-2}s$  (20000 MC steps) and  $t = 1.87 \times 10^{-2}s$  (1500 MC steps) simulation time, respectively. A central part of a much larger simulation area is presented. For  $E_{AB} < 0.08eV$  impurity decorated islands are formed.

Increasing or decreasing the temperature will only shift the boundary between these two types of structures and favor larger or smaller islands for the same number of deposited atoms.

Thesis 3: *In order to study not only qualitatively, but also quantitatively some material-related properties we developed the kMC method B, which uses the NEB method and the gEAM potential for calculating the hopping barrier of a diffusion process. Using this method I have studied the statistics of the diffusion of Pt atom clusters on a Pt(111) surface. The results obtained for the diffusion coefficient of different cluster sizes (up to  $N = 37$ ), are in agreement with those from the literature. I have found the leading microscopic mechanisms of the cluster diffusion process by studying the jump-size statistics of the clusters center of mass and the eccentricity of the clusters as a function of the temperature and cluster size. At low temperatures ( $T \leq 400K$ ) the cluster diffusion occurs by periphery diffusion of the atoms, while for higher temperatures ( $T \geq 700K$ ) the dissociation-recombination mechanism becomes more and more important.*

The kMC method B has the advantage relative to kMC method A that it can be used for quantitative studies on specific materials. As a verification for the method, first we used it to study the statistical properties of the diffusion of Pt atoms and clusters on a Pt(111) surface [3].

The Arrhenius relation (equation 1) holds for the diffusion coefficient for all cluster sizes.

$$D = D_0 \exp\left(-\frac{E_m}{k_B T}\right), \quad (1)$$

In (1),  $D_0$  is the pre-factor of the diffusion coefficient,  $E_m$  is a phenomenological activation energy (or sometimes called migration energy) of the diffusing particle or cluster,  $k_B$  is the Boltzmann constant, and  $T$  is the thermodynamic temperature of the system.

In agreement with experimental observations we assumed two possible mechanisms for cluster diffusion: a) Diffusion of atoms on the cluster edge (periphery diffusion), b) Dissociation of the cluster in two parts which can diffuse by their own, and recombine in a cluster with the original size. We also proposed a simple scaling argument for the size dependence of the diffusion coefficient's pre-factor ( $D_0$ ) in case of periphery diffusion, namely  $D_0 \sim N^{-1/2}$ .

From several simulation runs we computed an average diffusion coefficient ( $D$ ) for various cluster sizes ( $N = 1, 2, 3, 4, 5, 6, 7, 9, 13, 19, 25, 30$  and  $37$  atoms) and several system temperatures (from  $300K$  to  $900K$ ), using  $256 \times 256$  system size and no deposition flux ( $F = 0 \text{ ml/s}$ ).

The simulation results for the diffusion coefficient's pre-factor ( $D_0$ ) and the effective migration energy ( $E_m$ ) are in good agreement with those from FIM experiments [14], as shown in Fig. 5.

The  $D_0$  values determined from kMC simulations supports the proposed scaling property

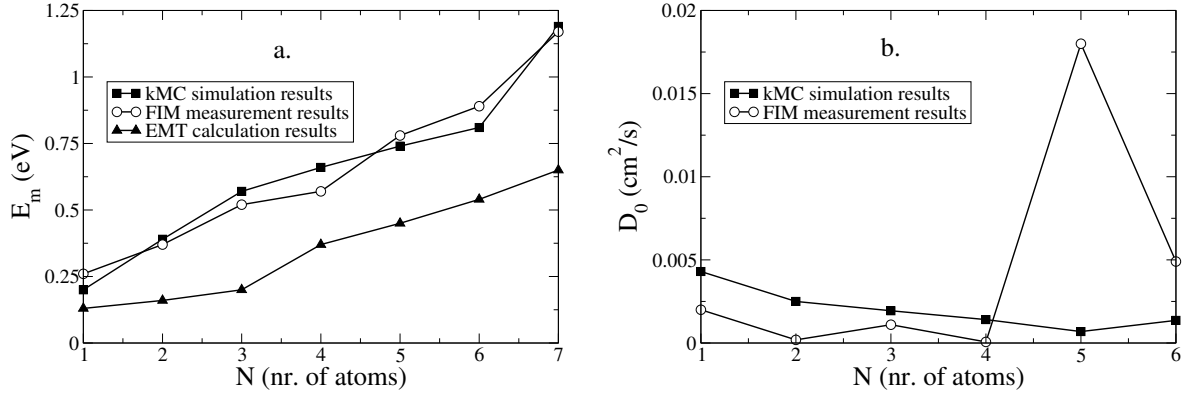


**Figure 5:** Simulation results for the values of the  $E_m$  migration energy (a) and for the  $D_0$  pre-factor of the diffusion coefficient (b) as a function of the cluster size,  $N$ , for  $N \leq 7$ .

$D_0 \sim N^{-1/2}$ . Plotting  $\log(D_0)$  as a function of  $\log(N)$  for simulations done at various temperatures leads to almost overlapping curves (Fig. 6). The general trends on this log-log plot suggest a scaling with an exponent very close to the theoretically predicted  $-0.5$  value. On Fig. 6 there are huge peaks observable for the closed shell configurations ( $N = 7$ ,  $N = 19$  and  $N = 37$ ) as several experimental and simulation studies [14, 15, 16] noticed. However, there is no final and conclusive theoretical explanation for its occurrence at the present.

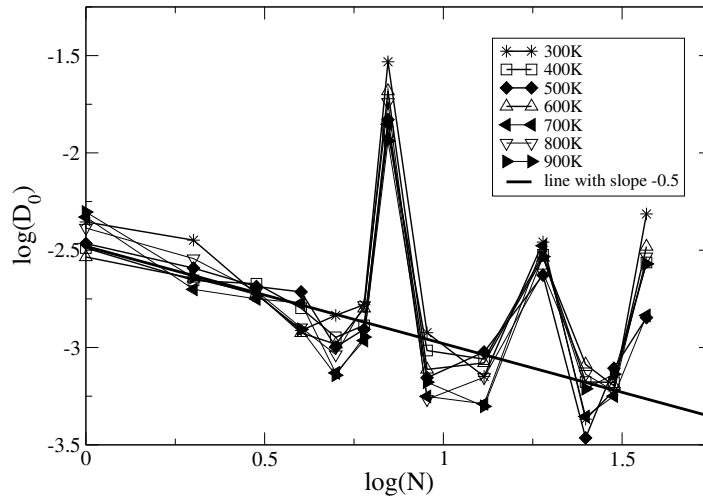


**Figure 6:** Size dependence of the  $D_0$  pre-factor of the diffusion coefficient.

By using computer simulations, the surface diffusion of the clusters can be approached on an event-by-event level, analyzing the individual displacements in the clusters Center of Mass (CM). Analyzing after each kMC event the absolute displacement of the CM and by determining their statistics, the results could yield additional information on the diffusion

process. From here on we use simply the term "jump" for the displacement of the CM in one simulation step. We measured the size of these jumps in lattice constant units for the open shell cluster:  $Pt_{13}$ .

By simple geometrical considerations one can state that jumps of sizes 0 occurs when a freely moving atom (an atom which escaped from the cluster) makes a diffusion step. In this case the CM of the cluster remains immobile for this time period. Jumps smaller than 0.12 lattice constants are characteristic for edge diffusion and jumps longer than 0.12 lattice constants are when an atom leaves the cluster or re-attaches to it. In case of periphery diffusion (jumps smaller than 0.12 lattice constants) one can observe jump sizes smaller than 0.07 lattice-constant when the edge atoms moves between an FCC and HCP site. If the periphery diffusion take places with a moving atom remaining on the FCC or HCP sub-lattice, the jump sizes will be between 0.07 and 0.12 lattice constant.

The jump size statistics performed at 300K, 500K, 700K and 900K is presented as simple histograms in Fig. 7.

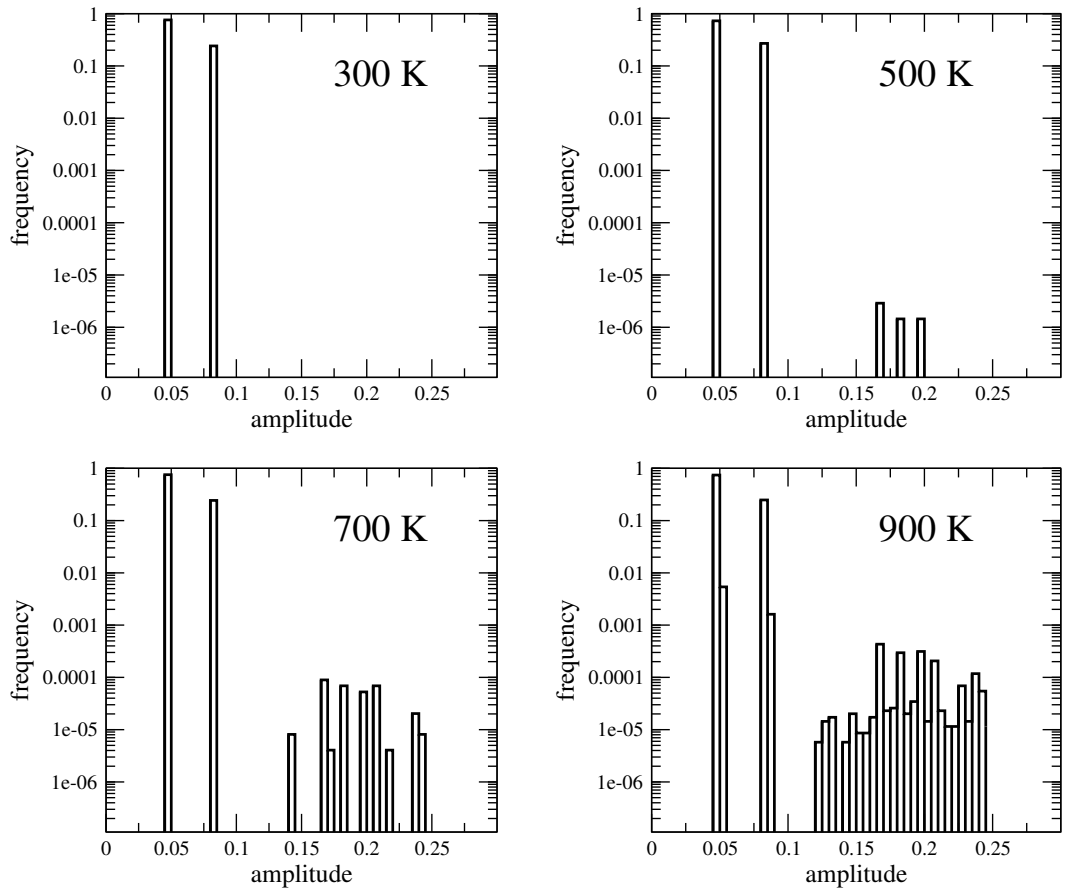


**Figure 7:** Jump-size statistics (histograms) for different temperatures. Please note the logarithmic vertical scale.

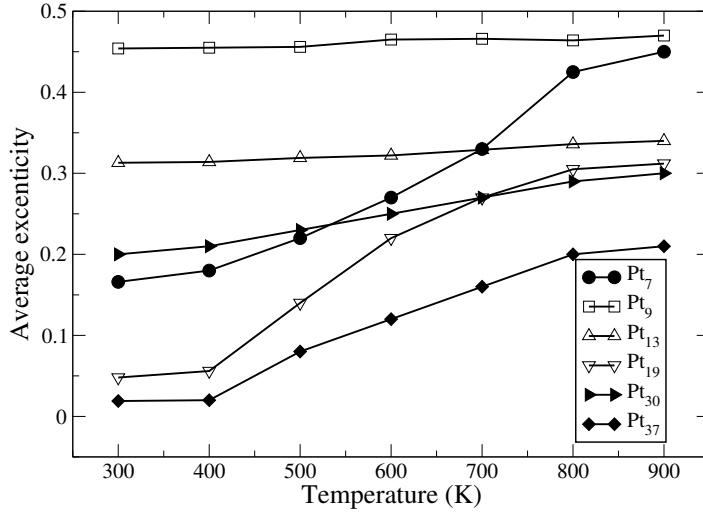


**Figure 8:** Average eccentricity of the  $Pt_7$ ,  $Pt_{13}$ ,  $Pt_{19}$ ,  $Pt_{25}$ ,  $Pt_{30}$  and  $Pt_{37}$  clusters as a function of the system temperature.

These histograms illustrate nicely the effect of temperature on the relative frequency of the main diffusion mechanisms in the model. At lower temperatures ( $T = 300K$ ) the edge diffusion mechanism is the leading one, since the jump sizes are mostly below 0.12 lattice constants. For higher temperatures ( $T = 700K$  and  $T = 900K$ ) the cluster fragmentation probability becomes higher, leading to jumps bigger than 0.12 lattice constants.

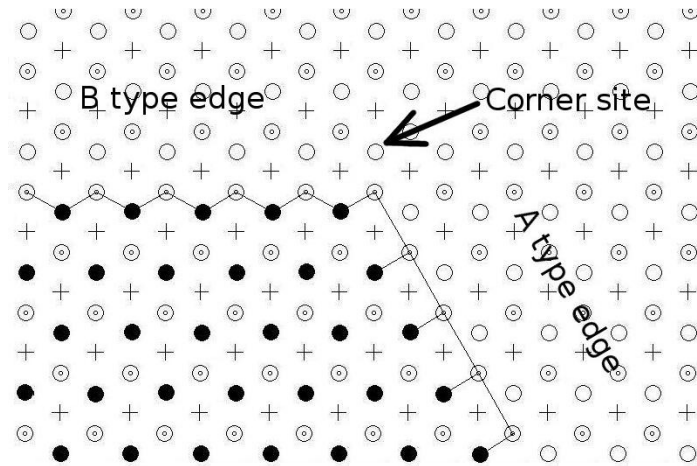
Using the result of the kMC simulations we also studied the time-averaged eccentricity ( $\varepsilon$ ) of the Pt clusters containing 7, 9, 13, 19, 30 and 37 atoms in a temperature range between  $T = 300K$  and  $T = 900K$ . The results are plotted in Fig. 8. As expected, the average eccentricity is always monotonically increasing with the temperature. The increased thermal fluctuations will distort the minimum energy disc-like configurations in increasing manner.

Fig. 8 also indicates that the considered clusters can be classified into two groups after their  $\varepsilon(T)$  trend. The first group contains clusters with eccentricities varying almost linearly as a function of temperature ( $N = 9, 13,$  and  $30$ ). The second group contains clusters with eccentricity values much smaller at low temperatures and with a non-linear (saturation-like) variation of the eccentricities as a function of temperature ( $N = 7, 19$  and  $37$ ). This second group contains the clusters with closed shell structures.

The reason of why the eccentricity of the smaller closed shell clusters are higher than for the bigger closed shell configurations is simple: the movement of an atom (a basic event in simulation) will influence in a larger manner the value of the eccentricity for smaller clusters than for the bigger ones.

Thesis 4: During the epitaxial deposition of Pt on the Pt(111) surface in a quite broad temperature and deposition flux range, just B type triangular-shaped 2D adatom islands are formed. Over the years several theoretical and experimental studies were done to explore the atomistic mechanism for the shape selection and orientation of the Pt islands on Pt(111) surfaces, but there is still no a consensus for it. Using the kMC method B, we shed new light on the origin, formation and stability of the oriented triangular Pt island on Pt(111) surface. I have studied the diffusion speed along the island edges (A- and B-type edges), the rates of edge to corner and corner to edge jumps and the kink formation and annihilation on the edges. We concluded that the atoms will populate the A-type edges with a higher probability, but the atoms will also assemble with a higher probability on these type of edges. These conditions leads to the quicker advancement and disappearance of the A-type edges, finally resulting in stable B-type triangular islands.

On the (111) surfaces of FCC metals the compact islands are bounded by two types of topologically non-equivalent steps (edges). These are the (100) microfacet (type A) and the (111) microfacet (type B), as illustrated in Fig. 9. During the epitaxial deposition of Pt on the Pt(111) surface only B type triangular 2D adatom islands are formed, at any temperatures.



**Figure 9:** Geometry of the A and B type edges. Dotted circles represents the sites of the substrate, circles and crosses represents the FCC and HCP lattice sites of the growing layer. The filled circles are the FCC sites of the growing layer which are already occupied by the adatoms.

Over the years several theoretical studies were done to explore the atomistic mechanism for the shape selection and orientation of the Pt islands on Pt(111) surfaces, but no convincing microscopic mechanism supporting these phenomenon was given.

As a first simulation step, we simulated the fast deposition of Pt atoms, by starting from a compact seed containing seven atoms. These islands (clusters) are already quite immovable,

as pointed out by Müller et al. [17]. Even for such high deposition fluxes as  $1000 \text{ ml/s}$ , the kinetic shapes of the simulated islands are compact and triangle-like, as can be seen in Fig. 10.

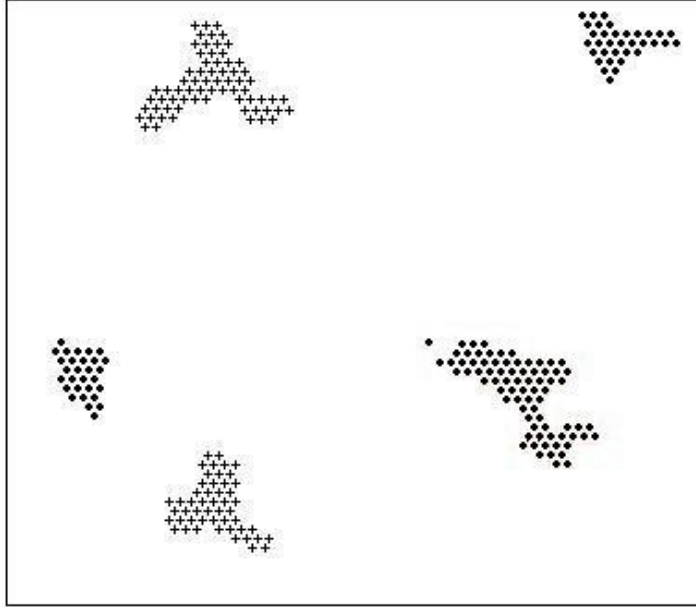


**Figure 10:** *kMC simulation results for  $1000 \text{ ml/s}$  adatom deposition flux at  $300\text{K}$  after 227 *kMC* steps (corresponding to a real time of  $4.3 \times 10^{-5} \text{ s}$ ). The simulated system size is  $64 \times 64 \times 4$ , disks and crosses represent the atoms in the growing layer occupying FCC and HCP lattice sites, respectively.*

Under such conditions the islands created with more than five atoms on the HCP sites are stable in time, in spite of the well-known fact that the FCC stacking islands are energetically more favorable than the HCP ones for Pt. The triangular-shaped FCC and HCP stacking islands are both B-type islands. Due to the topological differences for the two different stackings, the direction of the HCP triangles is just the opposite of the FCC triangles.

We realized a second study in order to verify the stability of islands of different types. A- and B-type FCC triangular islands formed by 21 atoms were considered and evolved using no deposition flux. As can be seen in Fig. 11, for all the simulated temperatures ( $300\text{K}$ ,  $400\text{K}$ ,  $500\text{K}$ , and  $600\text{K}$ ) the B-type triangular islands will keep their orientation or become truncated B-type triangles. This clearly does not hold for the A-type islands. The islands which are initially A type ones, are distorted at lower temperatures and even inverted to B-type triangles at higher temperatures.

Because the kMC method B reproduced the B-type triangular islands, for a better understanding of both the triangular-shaped island formation phenomenon and the higher stability of the B-type triangular islands, we calculated the characteristic energy barriers for the

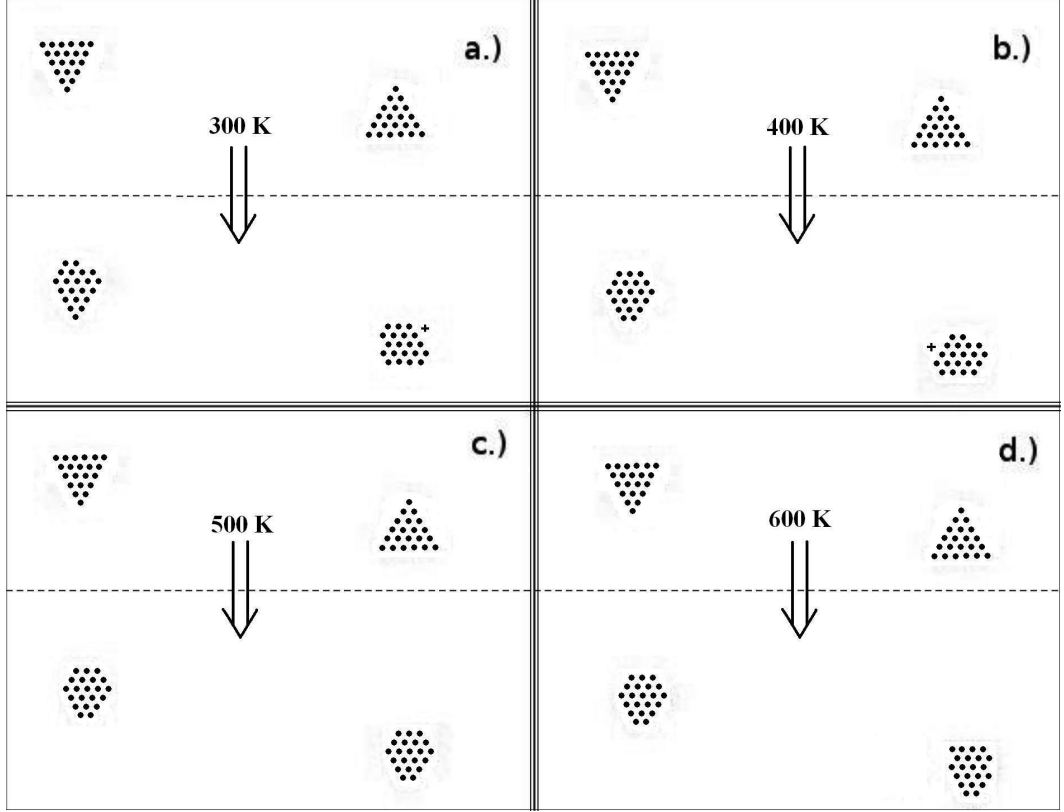


**Figure 11:** Time evolution of A (right) and B (left) type triangles without an external deposition flux. Each box indicates the initial (upper) and final (lower) configurations at different temperatures: (a) after 488 Monte Carlo steps corresponding to simulated time  $7.6 \times 10^{-2}$  s, at 300 K, (b) after 490 Monte Carlo steps  $6.9 \times 10^{-3}$  s, at 400 K, (c) after 149 Monte Carlo steps,  $1.4 \times 10^{-3}$  s, at 500 K, and (d) after 151 Monte Carlo steps,  $1.1 \times 10^{-4}$  s, at 600 K.

relevant microscopical events.

We computed the diffusion coefficient for single-atom diffusion on both A- and B-type edges. The results prove the validity of the Arrhenius relation in both cases and indicates for the A-type edge the effective (or apparent) migration energy  $E_m = 0.36 eV$  and for the pre-factor of the diffusion coefficient  $D_0 = 5.14 \times 10^{-3} cm^2/s$ . The values for the B-type edge are  $E_m = 0.6 eV$  and  $D_0 = 4.38 \times 10^{-3} cm^2/s$ .

Using the NEB method we calculated the energy barriers for edge to corner and corner to edge jumps. The values are:  $E_{A_1 \rightarrow 2} = 0.143 eV$ ,  $E_{A_2 \rightarrow 1} = 0.541 eV$  and  $E_{B_1 \rightarrow 2} = 0.370 eV$ ,  $E_{B_2 \rightarrow 1} = 0.767 eV$  respectively. The index numbers represents the number of nearest neighbors at the initial and final states of the jump.

From these results one can conclude that atoms on A-type edges will diffuse more easily than atoms on B-type edges and this holds not only along the edges, but also for jumps to and from the corners. These effects would favor a more rapid growth of the B-type edges and

ultimately the formation of A-type triangles, however, in experiment stable B-type islands are formed.

We considered further studies analyzing the kink-formation and kink-breaking phenomenon (Fig. 12).

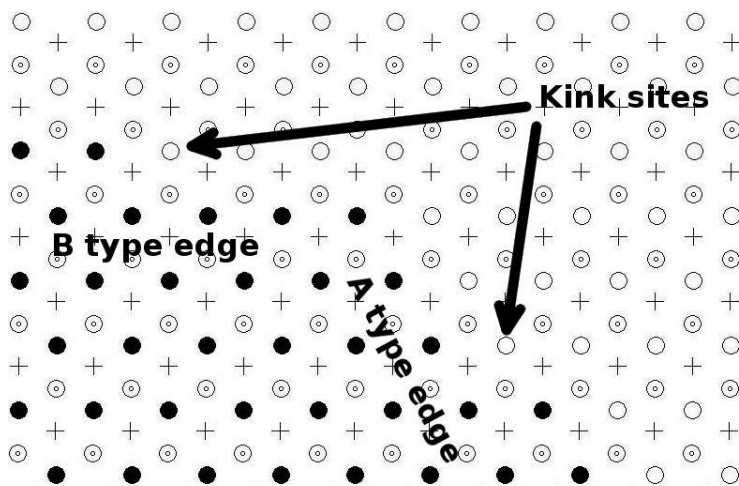


**Figure 12:** Kink sites on A and B type edges.

This is another elementary process in step advancement and therefore can be an important process in triangle-shape formation. The energy barriers calculated for kink-formation and kink-breaking events are:

$$E_{kink\ formation\ on\ A\ edge} = 0.281\ eV, E_{kink\ braking\ on\ A\ edge} = 0.624\ eV,$$

$$E_{kink\ formation\ on\ B\ edge} = 0.469\ eV, E_{kink\ braking\ on\ B\ edge} = 0.830\ eV.$$

Studying the energies necessary for kink formation and kink breaking reveals, however, that the atoms will assemble with a higher probability on A-type edges, leading to a higher advancement speed of the A-type steps. The higher jump probability from the corner sites to A-type edges leads also to a quicker advancement of A-type edges and ultimately to the formation of B-type triangular-shaped islands [4].

## Conclusions

The aim of my PhD research was to develop novel kinetic Monte Carlo methods and study some thin film related questions and problems with them. I developed two original kMC methods (method A and B).

The kMC method A, improves the classical method by using a new hopping barrier formula and more degrees of freedom for the diffusion of particles. With this fast kMC method, for the one component system, the island growth, the coalescence, and the appearance of stacking-faults related phase-boundaries and their motions were all successfully reproduced. For the two-component co-deposition process, impurity decorated islands were successfully modeled without using a predefined rate for the direct exchange of the neighboring different type particles.

The kMC method B performs a more accurate calculation of hopping barriers by using the Nudged Elastic Band method. The interaction of the particles are calculated with the generalized Embedded Atom Method. Using this method we could study material related properties like the diffusion of Pt atom clusters on a Pt(111) surface. Using event-by-event recording and following the eccentricity of the clusters as a function of the temperature and the cluster size, we found the leading microscopic mechanisms of the cluster diffusion process. At low temperatures ( $T \leq 400K$ ) the cluster diffusion occurs by periphery diffusion of the atoms, while for higher temperatures ( $T \geq 700K$ ) the dissociation-recombination mechanism becomes more and more important.

With kMC method B we also studied the origin, formation, and stability of the oriented triangular Pt islands on Pt(111) surface. Studying the diffusion of the atoms along the A and B type edges, the corner to edge and edge to corner jumps, and the kink formation and kink breaking energies, we revealed the origin for the formation and stability of the B-type triangular islands. The atoms will populate the A-type edges with a higher probability, but the atoms will also assemble with a higher probability on these type of edges. These conditions leads to the quicker advancement and disappearance of the A-type edges, finally resulting in stable B-type triangular islands.

My personal contributions to these studies were:

- writing ALL the simulation codes in C
- running the programs and performing the simulations
- making the graphs and figures for the publications
- contributing to the interpretation of the data
- helping in writing the publications

# Original contributions related to the dissertation

- [1] R. Deák and Z. Néda and P. B. Barna, "A Simple Kinetic Monte Carlo Approach for Epitaxial Submonolayer Growth", *Communications in Computational Physics*, vol. 3, pp. 822–833, 2008.
- [2] R. Deák and Z. Néda and P. B. Barna, "A novel kinetic Monte Carlo method for epitaxial growth", *Journal of Optoelectronics and Advanced Materials*, vol. 10, pp. 2445–2450, 2008.
- [3] R. Deák and Z. Néda and P. B. Barna, "A kinetic Monte Carlo approach for self-diffusion of Pt atom clusters on a Pt(111) surface", *Communications in Computational Physics*, vol. 10, pp. 920–939, 2011.
- [4] R. Deák and Z. Néda, "Kinetic Monte Carlo approach for triangular-shaped Pt islands on Pt(111) surfaces", *Physica Status Solidi B*, vol. 249, pp. 1709–1716, 2012.

## Selected bibliography

- [5] Peter M. Martin, *Handbook of Deposition Technologies for Films and Coatings (Third Edition): Science, Applications and Technology*, Elsevier Inc., 2010.
- [6] A. Cho, "Film Deposition by Molecular Beam Techniques", *Journal of Vacuum Science & Technology*, vol. 8, pp. S31–S38, 1971.

- [7] A. Cho and J. Arthur, "Molecular Beam Epitaxy", *Solid-State Chemistry*, vol. 10, pp. 157–192, 1975.
- [8] D. Kashchiev, *Nucleation: Basic Theory with Applications*, Oxford: Division of Reed Educational and Professional Publishing Ltd, 2000.
- [9] G. Mills and H. Jonsson, "Quantum and thermal effect in H<sub>2</sub> dissociative adsorption: Evaluation of free energy barriers in multidimensional quantum systems", *Physical Review Letters*, vol. 72, pp. 1124, 1994.
- [10] G. Henkelman and H. Jonsson, "Improved tangent estimate in the nudged elastic band method for finding minimum energy paths and saddle points", *Journal of Chemical Physics*, vol. 113, pp. 9978, 2000.
- [11] H. N. G. Wadley, X. Zhou, R. A. Johnson and M. Neurock, "Mechanism, models and methods of vapor deposition", *Progress in Materials Science*, vol. 46, pp. 329, 2001.
- [12] P. B. Barna, *Proc. 9th International Vacuum Congress, J. de Segovia (Ed.)*, Madrid, 1983, pp. 382–396.
- [13] R. Deák, Z. Néda and P. B. Barna, <http://phys.ubbcluj.ro/~zneda/kmc.htm>
- [14] K. Kyuno and G. Ehrlich, "Diffusion and dissociation of platinum clusters on Pt(111)", *Surface Science*, vol. 437, pp. 29–37, 1999.
- [15] S. C. Wang, U. Kurpick and G. Ehrlich, "Surface diffusion of compact and other clusters: Irx on Ir(III)", *Physical Review Letters*, vol. 81, pp. 4923–4926, 1998.
- [16] U. Kurpick, B. Fricke and G. Ehrlich, "Diffusion mechanisms of compact surface clusters: Ir<sub>7</sub> on Ir(111)", *Surface Science Letters*, vol. 470, pp. 45–51, 2000.
- [17] M. Muller, K. Albe, C. Busse, A. Thoma and Th. Michely, "Island shapes, island densities, and stacking-fault formation on Ir(111): Kinetic Monte Carlo simulations and experiments", *Physical Review B.*, vol. 71, pp. 075407-1, 2005.